



Journal of Applied Sciences

ISSN 1812-5654

science
alert

ANSI*net*
an open access publisher
<http://ansinet.com>



Research Article

Cadmium Removal from Aqueous Solution Using Superparamagnetic Iron Oxide Nanosorbents on Amberlite IR 120 H Support

¹Mohamed El-Sherif Goher, ²Mostafa Mahmoud Emara, ¹Mohamed Hassan Abdo, ³Nesrine Mohamed Refaat Mahmoud, ¹Amaal Mansour Abdel-Satar and ¹Amr Salah El-Shamy

¹Laboratory of Chemistry, Division of Freshwater and Lakes, National Institute of Oceanography and Fisheries (NIOF), Cairo, Egypt

²Department of Chemistry, Faculty of Science, Al-Azher University, Cairo, Egypt

³Department of Chemistry, Faculty of Pharmacy, Al-Nahda University, BaniSwaif, Egypt

Abstract

Background: Nanotechnology for water remediation is expected to play a crucial role in water security and consequently the food security of the world. Reactive nanoparticles have a significant amount of surfaces and thus attract much interest to be applied as adsorbents in comparison to macromolecules. This study aimed to use the nanoparticles as an inventive technique for the purification of water from heavy metals. **Materials and Methods:** Superparamagnetic iron oxide nanosorbents on resin amberlite IR 120 H support (SPION-AMIR) was used in a fixed-bed column system to remove cadmium ions from aqueous solution. Experimental study was carried out under several variables including the initial concentration (100-300 ppm), the amount of SPION-AMIR (0.5-3 g), flow rate (1-3 mL min⁻¹) and the pH (2-7) to indicate the breakthrough point and the removal efficiency of the nanosorbent. **Results:** By using 1 g of SPION-AMIR, the adsorption efficiency was recorded 307.04 mg g⁻¹ at the optimum conditions of pH 7, 200 ppm of Cd concentration and flow rate 1 mL min⁻¹. The isotherm study showed that the adsorption process fitted to Langmuir and Freundlich isotherms models with slight advantage for the Langmuir approach. Adsorption of Cd by SPION-AMIR follows the pseudo-second-order reaction. **Conclusion:** The obtained results demonstrated that SPION-AMIR can be used as excellent adsorbent to remove high amounts of cadmium from industrial wastewater.

Key words: Adsorption process, cadmium removal, isotherm model, kinetic model, nanosorbent, superparamagnetic

Received: January 29, 2017

Accepted: March 28, 2017

Published: May 15, 2017

Citation: Mohamed El-Sherif Goher, Mostafa Mahmoud Emara, Mohamed Hassan Abdo, Nesrine Mohamed Refaat Mahmoud, Amaal Mansour Abdel-Satar and Amr Salah El-Shamy, 2017. Cadmium removal from aqueous solution using superparamagnetic iron oxide nanosorbents on amberlite IR 120 H support. J. Applied Sci., 17: 296-305.

Corresponding Author: Mohamed El-Sherif Goher, Laboratory of Chemistry, Division of Freshwater and Lakes, National Institute of Oceanography and Fisheries (NIOF), Cairo, Egypt

Copyright: © 2017 Mohamed El-Sherif Goher *et al.* This is an open access article distributed under the terms of the creative commons attribution License, which permits unrestricted use, distribution and reproduction in any medium, provided the original author and source are credited.

Competing Interest: The authors have declared that no competing interest exists.

Data Availability: All relevant data are within the paper and its supporting information files.

INTRODUCTION

Cadmium (Cd) is one of the most toxic heavy metals, which may exist in water and wastewater. Cadmium has been recognized for its negative effects on the environment where it accumulates throughout the food chain posing serious threat to human health¹. Surface waters containing in excess of a few micrograms of cadmium per liter have probably been contaminated by industrial wastes from metallurgical plants, plating works, plants manufacturing cadmium pigments, textile operations, cadmium-stabilized plastics, nickel-cadmium batteries or by effluents from sewage treatment plants². The recommended amount of cadmium ion in drinking water sources according to WHO³ is 10 µg L⁻¹. Treatment of water by conventional methods such as precipitation with lime and treatment with alum and ferric sulfate is not suitable to remove it and also is less effective⁴. According to Ilankoon⁵, different treatment technologies are available for the removal of toxic heavy metals. The adsorption⁶, chemical precipitation⁷, ion exchange⁸, coagulation⁹, reverse osmosis¹⁰, electrolysis and membrane process¹¹ are widely used. However, among all of these methods, adsorption is considered as one of the most effective, efficient and economical method for the removal of pollutants from wastewater^{12,13}.

Surface waters containing in excess of a few micrograms of cadmium per litre have probably been contaminated by industrial wastes from metallurgical plants, plating works, plants manufacturing cadmium pigments, textile operations, cadmium-stabilized plastics, or nickel cadmium batteries or by effluents from sewage treatment plants.

Nanotechnology for water remediation is expected to play a crucial role in water security and consequently the food security of the world¹⁴. In recent years, a great deal of attention has been focused on the synthesis and application of nanostructure materials as adsorbents to remove toxic and harmful substances from industrial wastewater. Resurgence to synthesize and manipulate nanoparticles finds use in improving water quality in the environment¹⁵. Applications of nanotechnology could be summarized in the cleanup of wastewater as: (1) Nanoscale filtration techniques, (2) The adsorption of pollutants on nanoparticles and (3) The breakdown of contaminants by nanoparticle catalysts¹⁴.

Reactive nanoparticles have a significant amount of surfaces and thus attract much interest to be applied as adsorbents in comparison to macromolecules¹⁵. Metal oxides play a significant role in many fields of nanotechnology

including superparamagnetic properties^{16,17}. Iron oxides exist in different forms in nature, as magnetite (Fe₃O₄), hematite (α-Fe₂O₃) and maghemite (γ-Fe₂O₃)¹⁸. The surface effects have a strong influence on the magnetic properties of iron oxide nanoparticles¹⁹. Iron oxide (Fe₃O₄) superparamagnetic nanomaterials have unique properties, such as diminished consumption of chemicals, larger surface area-volume ratio and no secondary pollutant. However, with another special property of this kind magnetic materials are often employed in the context of environmental remediation. More and more magnetic separation has been combined with adsorption for the removal of cadmium from contaminated water at laboratory scales^{20,21}. In addition, the adsorption is sometimes reversible and adsorbent can be regenerated by suitable desorption process²². In this study, the effect of nanosorbent and acidic resin combination on the efficiency of metal removal was assessed.

The main objective of this study was to remove cadmium from aqueous solution using newly developed SPION-AMIR. A detailed investigation on the initial concentration (100-300 ppm), the mass of adsorbent (0.5-3 g), the contact time (1-3 mL min⁻¹) and the solution pH (2-7) on Cd ions removal from a solution was carried out. Number of bed value at 100% removal and breakthrough for SPION-AMIR were determined. Isotherm and kinetic studies were used to quantify the adsorption process.

MATERIALS AND METHODS

Preparation of aqueous solution: A stock solution of Cd ions was prepared by dissolving a known quantity of Cd(NO₃)₂·4H₂O in deionized water. After the adsorption process, the residual metals in solution were analyzed, using GBC atomic absorption reader (Model SavantAA AAS with Flame and GF 5000 Graphite Furnace). The pH was adjusted by using 1.0 M NaOH and 1.0 M HCl²³.

Characterization of adsorbent: The characteristics of SPION-AMIR are synthesized with particle size ranging 33.2-2.9 nm (<100 nm). The shape, porous and size of the synthesized nanoparticles were confirmed using SEM, XRD and FTIR. The magnetization property of SPION-AMIR was confirmed using Magnetic Susceptibility Balance (MSB) to give the effective magnetic moment (μ_{eff}) which equal 31.31 emu mol⁻¹. Successful exploitation of metallic nanoparticles lies in the successful conjugation of their active surface structure. Thus, size and shape play a role in terms of

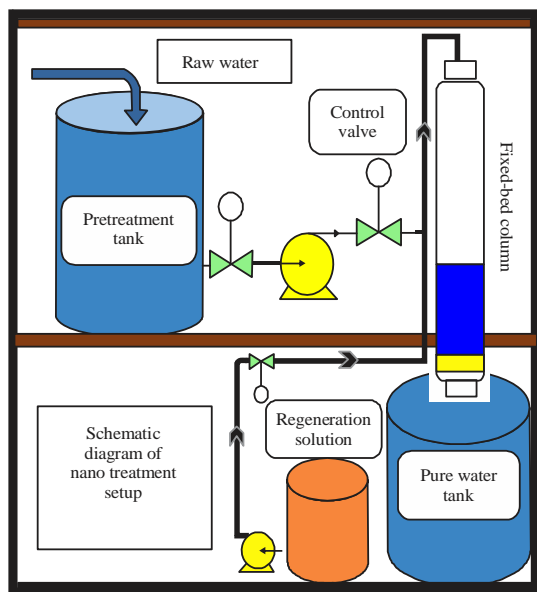


Fig. 1: Schematic diagram of fixed-bed column setup

variable surface energy. Emara *et al.*²⁴ described the details of SPION-AMIR properties.

Fixed-bed sorption process: A fixed-bed column runs were carried out using glass columns a small (in-out) constant flow water pump connected to a power supply of 9 V. Then water goes into the column runs using the constructed system (Fig. 1) which consists of a glass column (11 mm in diameter) and the flow-rate for all runs was adjusted to the required one. About 5 L feed solution containing a single pollutant under investigation was prepared from grade reagents and deionized water. About 5 mL aliquot from the effluent was analyzed regularly until the breakthrough is reached²⁵ using GBC atomic absorption reader (SavantAA AAS with GF 5000 Graphite Furnace).

The calculations were based on bed volumes and number of bed volumes. This methodology will help determine the adsorbent capacity of removing the pollutants cadmium ions under investigation depending on how much of water (mL) passed through the adsorbent bed. Equation 1 was used to calculate the bed volume:

$$B.V. = \pi r^2 h \quad (1)$$

where, B.V. is bed volume, π is 3.14, r is radius of column which is equal to 5.5 mm and h is height of exchanger in the column. In addition, the number of bed volumes can be calculated by Eq. 2:

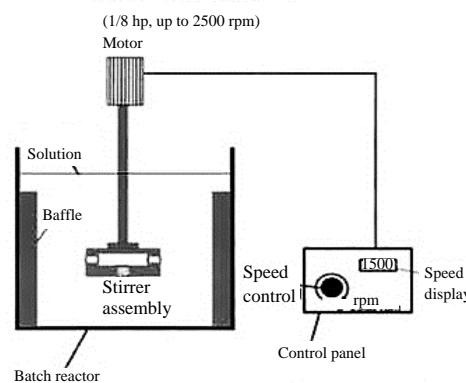


Fig. 2: Schematic of the batch kinetic test apparatus and reactor-stirrer assembly. Source: DeMarco *et al.*²⁷

$$\text{No. of B.V.} = (\text{Time of treated water passed} \times \text{flow rate}) / (B.V.) \quad (2)$$

The breakthrough value refers to the total number of bed volumes passed through the SPION-AMIR at that, the regeneration of the adsorbent is necessary (in the present study, the breakthrough was represented, when concentration of Cd in the treated water reached to the half value of the initial concentration). This can be determined from plotting the concentration ratio (C/C_0) of pollutant against bed volume²⁶.

Batch adsorption studies: Series of batch experiments were conducted for each experiment. About 50 mL of synthetic water sample of 2 mg L⁻¹ cadmium ions at pH = 7 and temperature (T) of 25 ± 1 °C for 120 min on a set-up shown in Fig. 2 were loaded within the cell of the stirrer and was stirred at 150 rpm. When the stirrer assembly rotates, the centrifugal action produces a rapid circulating flow of solution entering the cage at the bottom and leaving through the radial holes of the caging. Thus, a vigorous hydrodynamic condition surrounding the SPION-AMIR beads is maintained²⁷. A known volume (50 mL) each was pipette into the series of cultural vial to which (0.0005, 0.001, 0.005, 0.01, 0.05 g L⁻¹) of the SPION-AMIR as adsorbent was added. Upon completion of the given contact time (50-55 min) between adsorbent and adsorbate, the solution was filtered. The removal percentage (R%) can be calculated using Eq. 3:

$$R\% = \frac{(C_0 - C_e)}{C_0} \times 100 \quad (3)$$

where, C_0 and C_e are concentration (mg L⁻¹) of metal ions in the initial and equilibrium solutions, respectively. The equilibrium adsorption capacity (q_e) of each sorbent was calculated as shown in Eq. 4:

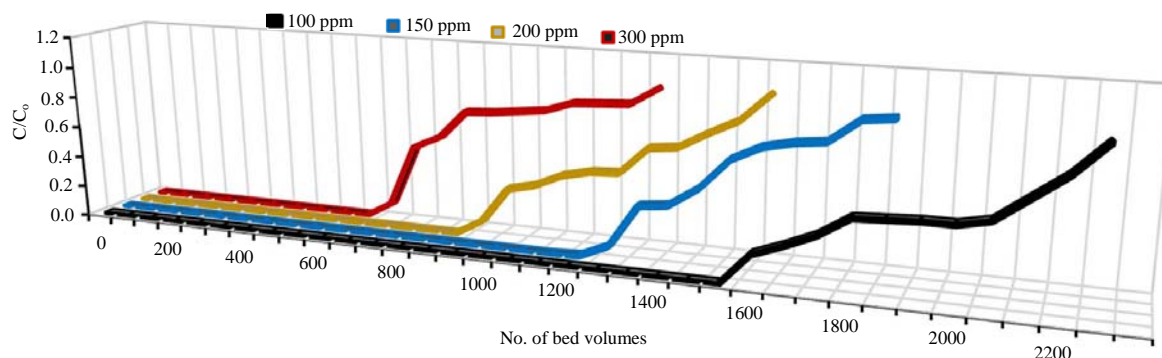


Fig. 3: Relation between removal percentage or concentration ratio (concentration of outflow solution C /initial concentration of inflow solution C_0) and number of bed volumes at different initial concentrations (100, 150, 200 and 300 ppm Cd) using 1 g of SPION-AMIR in a fixed bed column at pH 7 and flow rate 2 mL min^{-1}

$$q_e = \frac{(C_0 - C_c)V}{W} \quad (4)$$

where, V is the volume of the initial solution taken for equilibrium (L) and W is mass of the sorbent of the SPION-AMIR taken for equilibrium (g)²⁵.

RESULTS AND DISCUSSION

Effect of initial contaminant concentration: The effect of initial different Cd ions concentration (100, 150, 200 and 300 ppm) at 1 g of SPION-AMIR was studied and the flow rate was adjusted to be 2 mL min^{-1} . An influent solution with pH = 7 at $T = 25 \pm 1^\circ\text{C}$ was passed through a fixed bed column. The obtained results indicated complete removal of cadmium at number bed volume (B.V.) of 1509, 1200, 953 and 613 mL for 100, 150, 200 and 300 ppm of Cd concentration, respectively (Fig. 3).

On the other hand the breakthrough recorded at 2063, 1458, 1222 and 708 mL bed volumes, for 100, 150, 200 and 300 ppm of Cd concentration. It is worth mentioning that the increase in the initial concentration decrease the number of bed volume. On the other side, the adsorption capacity (q_e) of SPION-AMIR up to 114.68, 136.80, 144.86 and 139.76 mg g^{-1} for 100, 150, 200 and 300 ppm of Cd concentration, respectively. The adsorption capacity (q_e) increased by increasing the Cd concentration from 100-200 mg L^{-1} , further increasing of Cd ions to 300 mg L^{-1} led to decreasing the adsorption capacity. This may be due to the lack of available adsorbent sites at higher concentrations and hence, the percentage adsorption of cadmium decreases²⁸.

Flow rate (retention time): Investigation of changing contact time on the removal of Cd ions was studied using an influent solution of 200 ppm Cd at pH = 7, $T = 25 \pm 1^\circ\text{C}$ passed through a fixed bed column containing 1.00 g of SPION-AMIR at different rates (1, 2 and 3 mL min^{-1}). Figure 4 shows that the number of B.V. at 100% removal and breakthrough reach up to 1010, 953 and 641; 1249, 1222 and 681 bed volumes, respectively. A reverse relation between the adsorption process and the increasing of flow rate is reported by Khalilnezhad *et al.*²⁹. On the other hand, the adsorption capacity (q_e) values were 307.04, 144.86 and 64.95 mg g^{-1} for 1, 2 and 3 mL min^{-1} , respectively. The present results are in harmony with those obtained by Kamarudzaman *et al.*³⁰, who described that the decrease of metal removal at higher flow rate may be attributed to insufficient contact time of the metal ions in the column. Where, the metal ions did not have enough time to diffuse into the pores of the sorbent and leaving the column before equilibrium was achieved.

Mass of adsorbent: The effect of SPION-AMIR mass on the removal cadmium ions from water was studied to get the optimum conditions for the removal process. For this purpose different masses of adsorbent (0.5, 1, 2 and 3 g) were applied for the removal of cadmium ions using solutions of concentration (200 ppm Cd) at flow rate 2 mL min^{-1} , pH = 7 and $T = 25 \pm 1^\circ\text{C}$ each in a fixed bed column run. The number of B.V. at 100% removal value was recorded at 733, 953, 909 and 706 mL min^{-1} for 0.5, 1, 2 and 3 g of SPION-AMIR, respectively. On the other hand, the breakthrough was observed after 1046, 1222, 1183 and 1211 mL min^{-1} for 0.5, 1, 2 and 3 g of SPION-AMIR, respectively (Fig. 5). According to

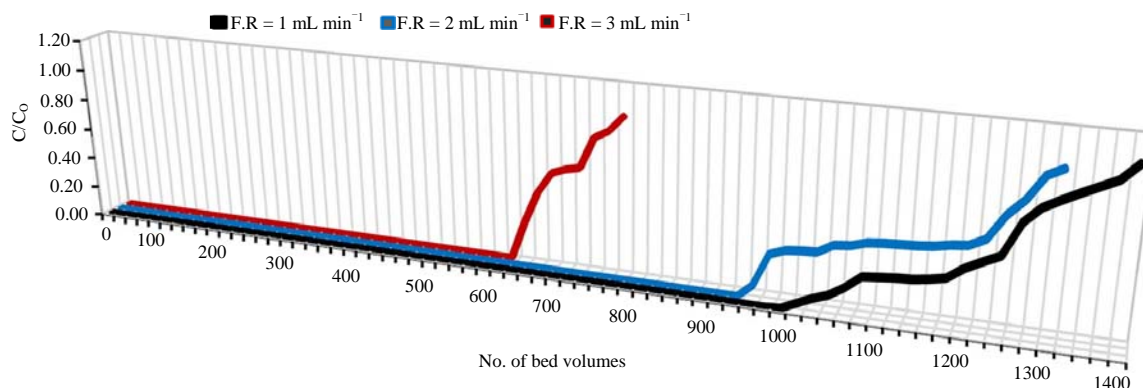


Fig. 4: Relation between removal percentage or concentration ratio (concentration of outflow solution C /initial concentration of inflow solution C_0) and number of bed volumes at different flow rate (1, 2 and 3 mL min⁻¹) using 1 g of SPION-AMIR in a fixed bed column at pH 7 and initial concentration of 200 ppm Cd

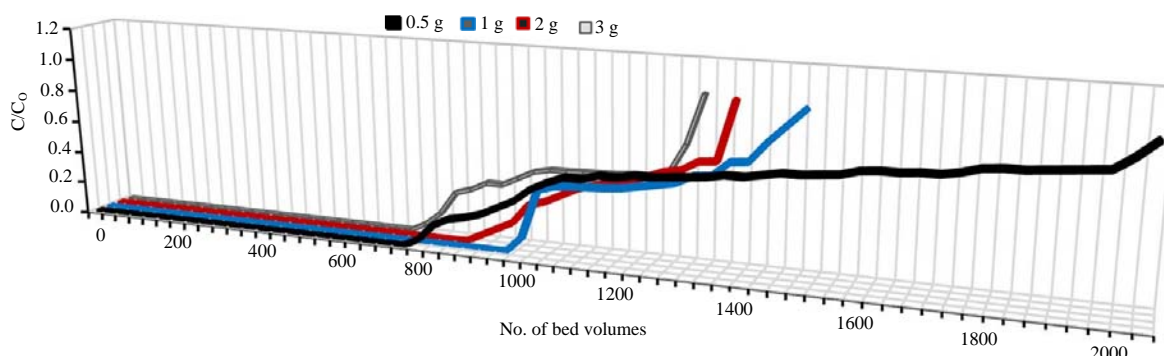


Fig. 5: Relation between removal percentage or concentration ratio (concentration of outflow solution C /initial concentration of inflow solution C_0) and number of bed volumes using different mass of adsorbent SPION-AMIR (0.5, 1, 2 and 3 g) in a fixed bed column at pH 7, flow rate 2 mL min⁻¹ and initial concentration of 200 ppm Cd

Eq. 4, the adsorption capacity values (q_e) using 0.5, 1, 2 and 3 g of SPION-AMIR recorded 125.34, 144.86, 146.80 and 111.78 mg g⁻¹, respectively.

The results indicated that the increase of the mass of SPION-AMIR increase the removal of cadmium ions, where, the number of adsorption sites was increased and consequently the removal of Cd improved. The determination of effect of adsorbent dosage gives an idea about the minimum amount of adsorbent need to be used for adsorption process. This value is useful in the viewpoint of cost³¹. Generally, the increase of mass adsorbent and the bed height, which provided much sorption sites for Cd ions, longer contact time of Cd ions in the column and therefore delivered better intra-particle phenomena^{29,32}.

Effect of solution pH: The pH of the solution is an important parameter, which controls the adsorption process. It influences the ionization of the adsorptive molecule and hence the surface charges of the adsorbent. The pH effect on the removal process of 200 ppm Cd ions was studied using 1 g of SPION-AMIR at 2 mL min⁻¹ flow rate with $T = 25 \pm 1^\circ\text{C}$ at pH = 2, 4 and 7. At pH = 2.0, the number of B.V. at 100% removal value was 434 and breakthrough was observed after 485 bed volumes, while, the number of B.V. at 100% removal value was 609 and breakthrough was observed after 759 bed volumes at pH = 4 and finally at pH = 7 the number of B.V. at 100% removal value was 953 and breakthrough was observed after 1222 bed volumes (Fig. 6). The adsorption capacity (q_e) values were 65.97, 92.57 and 144.86 mg g⁻¹ for pH 2, 4 and 3,

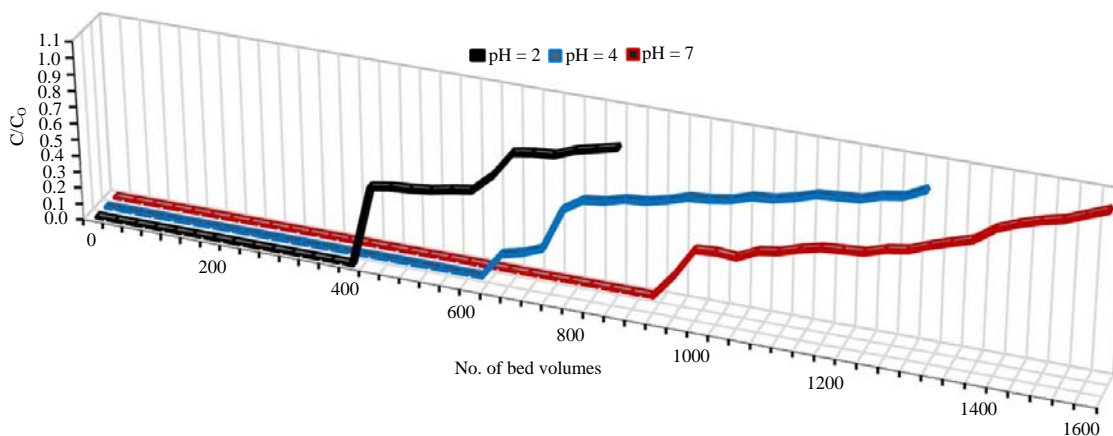


Fig. 6: Relation between removal percentage or concentration ratio (concentration of outflow solution C/initial concentration of inflow solution C₀) and number of bed volumes at different pH (2, 4 and 7) using 1 g of SPION-AMIR in a fixed bed column at flow rate 2 mL min⁻¹ and initial concentration of 200 ppm Cd

Table 1: Kinetic parameters for the removal of cadmium using SPION-AMIR

Metal	Pseudo-first-order kinetic model				Pseudo-second-order kinetic model			
	K	R ²	q _e cal	q _e exp	K	R ²	q _e cal	q _e exp
Cd	0.047	0.953	1.186	9.091	0.085	0.9999	9.268	9.091

cal: Calculated, exp: Experimental

respectively. At low pH values, the cadmium removal decreased because the competition between H⁺ and cadmium ions for the adsorption sites, due to the high H⁺. On the other side, when the pH of the adsorbing medium increased from 4-7, there was a corresponding increase in the de-protonation of the adsorbent surface, leading to a decrease in H⁺ ions on the adsorbent surface³³. Furthermore at higher pH values (at pH>7) may be related to the precipitation of metals in the form of metal hydroxide due to the reaction of metal ions with OH⁻ as the amount of OH⁻ increases at high pH³⁴.

Several factors can affect the adsorption process, such as initial contaminant concentration solution, flow rate, adsorbent dosage and pH value and presence of other co-existing ions. In addition to these factors, the nanoparticle size and shape also affect to the adsorption performance²⁷. Higher adsorption capacities can be obtained by optimizing above parameters. The obtained results showed that the removal of cadmium up to 100% using 1 g of SPION-AMIR. Where, the maximum adsorption efficiency recorded 307.04 mg g⁻¹ at the optimum conditions of 200 ppm of Cd as an initial concentration of solution, pH 7 and flow rate 1 mL min⁻¹.

Kinetics studies: Kinetic performance of a given adsorbent is important to get an indication about the solute uptake rate. It determines the residence time required to complete the

adsorption reaction²⁷. Due to the importance, the kinetic studies have been performed in majority of studies^{28,35}. The pseudo first-order and pseudo second-order models developed by Ho *et al.*³⁶ connected with the reaction based models, different two kinetic models were applied to determine the mechanism involved in adsorption process.

Pseudo-first and second-order kinetic model: The sorption kinetics³⁷ may be described by a pseudo first order equation and represented by the non-linear Eq. 5 as:

$$\frac{dq_t}{dt} = K_1 (q_e - q_t) \quad (5)$$

where, q_e and q_t are the Cd concentrations (mg g⁻¹) in solid phase at equilibrium and at time t, respectively. K₁ is the rate constant for the pseudo-first-order adsorption process (L min⁻¹). It can be simplified and expressed in linearized form as shown in Eq. 6:

$$\log (q_e - q_t) = \log q_e - \frac{K_1}{2.303} t \quad (6)$$

The equilibrium experimental data were plotted between log (q_e-q_t) and t as shown in Fig. 7 for the removal Cd. The correlation coefficients (R²) and the model parameters were evaluated and given in Table 1.

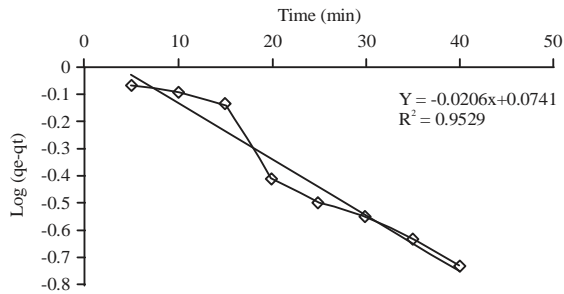


Fig. 7: Pseudo-first-order kinetic model plots for the removal of cadmium using SPION-AMIR

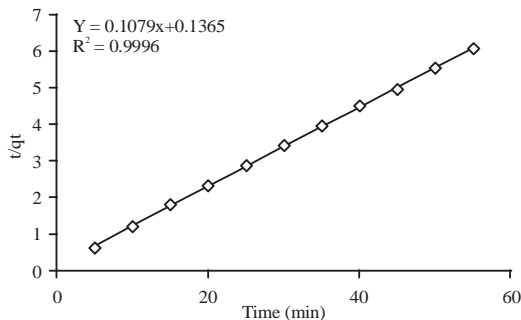


Fig. 8: Pseudo-second-order kinetic model plots for the removal of cadmium using SPION-AMIR

A pseudo-second-order kinetic model³⁶ is also utilized to explain the kinetic behavior of the operation. The applicability of the second-order kinetics is represented by Eq. 7:

$$\frac{dq_t}{dt} = K_2 (q_e - q_t)^2 \quad (7)$$

where, k_2 is the pseudo-second order rate constant of adsorption in ($g\ mg^{-1}\ min$), q_e and q_t is the amount of adsorbate adsorbed onto the adsorbent at equilibrium time and t time respectively, in ($mg\ g^{-1}$) and t is the contact time in minutes. It can be simplified and expressed in linearized form as shown in Eq. 8:

$$\frac{1}{(q_e - q_t)} = \frac{1}{q_e} + K_2 t \quad (8)$$

The equilibrium experimental data were plotted between $1/(q_e - q_t)$ and t as shown in Fig. 8 for the removal of cadmium. The correlation coefficients (R^2) and the model parameters were evaluated and given in Table 1.

Table 1 shows the calculated adsorption capacity of 1.186 and 9.091 $mg\ g^{-1}$ for pseudo-first order and pseudo-second order models compared to the experimental one of 9.086. The obtained values of correlation coefficients (R^2); 0.956 and 0.9996 for pseudo-first order and

pseudo-second order, respectively; in addition to the values of the experimental q_e which is closed to the calculated q_e of pseudo-second order rate, suggests the applicability of pseudo-second order kinetics for the adsorption of Cd onto the SPION-AMIR adsorbent. The evaluation of the kinetic constants is important for the designing of the fixed bed adsorption column, as it will also provide the idea about the rate of adsorption. The various design parameters for the fixed-bed adsorption column such as the breakthrough time and the shape of the breakthrough curve are dependent on the rate of adsorption. If the rate of adsorption is fast, the shape of the breakthrough curve would be steep and the fraction of utilized bed would be higher. It was found that the rate of the adsorption was high at the beginning due to the availability of surface functional groups of the SPION-AMIR. As the surface functional groups become exhausted, the rate of sorption is controlled by the rate of transport from the external to the internal sites³⁸.

Adsorption isotherm model: Adsorption models of Langmuir and Freundlich were applied to determine the relationship of cadmium adsorption with different induced concentration. The best-fitting isotherm was evaluated by linear regression and the parameters obtained from the intercept and slope of the linear plots of these models.

Langmuir isotherm model: Estimation of maximum adsorption capacity corresponding to complete monolayer coverage on the nanomaterials was calculated using the Langmuir isotherm model since the saturated monolayer isotherm can be explained by the non-linear Langmuir Eq. 9 as:

$$q_e = \frac{q_{max} K_{\alpha} C_e}{1 + K_{\alpha} C_e} \quad (9)$$

The Langmuir isotherm model is assumes the formation of monolayer during the removal of cadmium metal from aqueous solution using developed SPION-AMIR adsorbent. The Langmuir isotherm study also provides the maximum adsorption capacity of the adsorbent for the removal of heavy metal ions³⁹. The linearized Langmuir isotherm model is expressed as Eq. 10:

$$\frac{1}{q_e} = \frac{1}{q_{max}} + \left(\frac{1}{q_{max} K_{\alpha}}\right) \left(\frac{1}{C_e}\right) \quad (10)$$

where, q_e is the adsorption capacity adsorbed at equilibrium in $mg\ g^{-1}$. C_e is the equilibrium concentration of adsorbate in the solution in milligram per litre, q_{max} is the maximum adsorption capacity in $mg\ g^{-1}$ (is the maximum quantity of

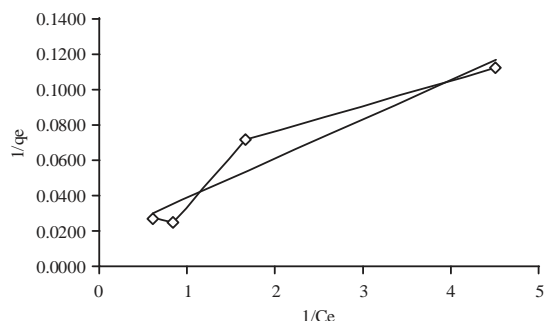


Fig. 9: Langmuir isotherm model plots for the removal of cadmium using SPION-AMIR

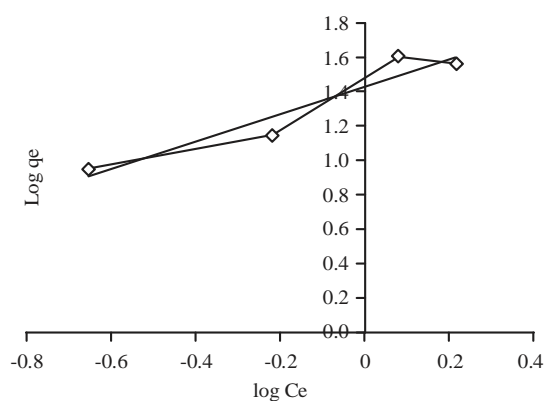


Fig. 10: Freundlich isotherm model plots for the removal of cadmium using SPION-AMIR

adsorbate required to form a single monolayer on unit mass of adsorbent (mg g^{-1}) and K_a is the Langmuir isotherm constant in L mg^{-1} (adsorption equilibrium constant). The equilibrium experimental data are plotted between $1/q_e$ and $1/C_e$ as shown in Fig. 9 for the removal of Cd. The correlation coefficients and the model parameters were evaluated and given in Table 2.

The degree of suitability of SPION-AMIR for the sorption of Cd ion was also estimated from the values of the separation factor constant (R_L) according to Eq. 11:

$$R_L = (1)/(1 + K_a C_0) \tag{11}$$

The value of $R_L > 1$ indicates unfavorable, $R_L = 1$ linear, $0 < R_L < 1$ favorable or $R_L = 0$ irreversible sorption. The R_L values for the sorption of Cd on SPION-AMIR are favorable and presented in Table 2.

Freundlich isotherm model: The Freundlich model suggests a heterogeneous adsorption of the solute on the adsorbent surface³¹. The model non-linear equation is expressed as Eq. 12:

$$q_e = K_f C_e^{\frac{1}{n}} \tag{12}$$

where, K_f is representing the Freundlich constant, which indicates the relative adsorption capacity of the adsorbent related to the bonding energy in mg g^{-1} and n is the heterogeneity factor representing the deviation from linearity of adsorption and is also known as Freundlich coefficient. It can be stated that, if the $1/n$ value is below unity, this implies that the adsorption process is chemical; if the value is above unity, adsorption is a favourable physical process⁴⁰. The Freundlich equation can be linearized⁴¹ and expressed as Eq. 13:

$$\log q_e = \log K_f + \frac{1}{n} \log C_e \tag{13}$$

The experimental data were plotted between $\log q_e$ and $\log C_e$ and shown in Fig. 10 for the removal of Cd. The coefficients for Freundlich isotherm were evaluated (Table 2).

The sorption data fitted for both Langmuir and Freundlich isotherms with high regression value (R^2) of 0.913 and 0.912, respectively. The Langmuir isotherm model suggests that the adsorption is primarily governed by the formation of the monolayer on the adsorption sites. The adsorption process fitted to Langmuir and Freundlich isotherms models with slight advantage for the Langmuir approach that is in agreement with that obtained by Bhargavi *et al.*⁴².

The obtained results of the experimental data as well as the kinetics study and the isotherm models confirmed that SPION-AMIR is an effective adsorbent for removal Cd from the wastewaters.

Table 2: Isotherm parameters for the removal of cadmium using SPION-AMIR

Metal	Langmuir isotherm model				Freundlich isotherm model			
	K_a	R^2	R_L	q_{max}	n	R^2	K_f	$1/n$
Cd	0.757	0.913	0.398	59.524	1.253	0.912	27.064	0.798

CONCLUSION

Novel superparamagnetic iron oxide nanosorbent on resin (Amberlite IR 120 H) support was used to remove Cd from aqueous solution. The fixed bed column experiment resulted in the maximum adsorption efficiency of 307.04 mg g⁻¹ at the optimum conditions of pH 7, Cd concentration (200 ppm) and flow rate 1 mL min⁻¹ using 1 g of SPION-AMIR. The adsorption of cadmium with SPION-AMIR follows the pseudo second-order kinetics. The adsorption process was fitted to Langmuir and Freundlich adsorption isotherm models. The values of adsorption intensities ($0 < R_L < 1$) indicate that the adsorption of cadmium with SPION-AMIR is favorable and it is good sorbent for cadmium ions. So, the present results declared that the superparamagnetic iron oxide nanosorbent is effective adsorbents and can be beneficial for removal of heavy metals from industrial waste and to use in water purification process.

SIGNIFICANCE STATEMENTS

This study discovered the high efficiency of combined nanosorbents with resins to remove high amounts of metals from wastewater that can be beneficial for the treatment methods and process of water purification. This study will help the researcher to uncover the critical areas of heavy metal remediation in wide economic scale that many researchers were not able to explore. Thus, a new theory on the combination effect of novel nanosorbents and ion exchanger/sorbent resin may be arrived at.

ACKNOWLEDGMENT

The authors would like to thank the Laboratory of Chemistry, Division of Freshwater and Lakes, NIOF and Department of Chemistry, Faculty of Science, Al-Azhar University for supporting this study.

REFERENCES

1. Pan, B., H. Qiu, B. Pan, G. Nie and L. Xiao *et al.*, 2010. Highly efficient removal of heavy metals by polymer-supported nanosized hydrated Fe (III) oxides: Behavior and XPS study. *Water Res.*, 44: 815-824.
2. Naja, G.M. and B. Volesky, 2009. Toxicity and Sources of Pb, Cd, Hg, Cr, As and Radionuclides in the Environment. In: *Heavy Metals in the Environment*, Wang, L.K., J.P. Chen, Y.T. Hung and N.K. Shamma, (Eds.). CRC Press, Taylor and Francis, Boca Raton, London, New York.
3. WHO., 2011. Guidelines for Drinking Water Quality. 4th Edn., World Health Organization, Geneva.
4. Ehrampoush, M.H., M. Miria, M.H. Salmani and A.H. Mahvi, 2015. Cadmium removal from aqueous solution by green synthesis iron oxide nanoparticles with tangerine peel extract. *J. Environ. Health Sci. Eng.*, Vol. 13. 10.1186/s40201-015-0237-4.
5. Ilankoon, N., 2014. Use of iron oxide magnetic nanosorbents for Cr (VI) removal from aqueous solutions: A review. *Int. J. Eng. Res. Applic.*, 1: 55-63.
6. Yang, W., P. Ding, L. Zhou, J. Yu, X. Chen and F. Jiao, 2013. Preparation of diamine modified mesoporous silica on multi-walled carbon nanotubes for the adsorption of heavy metals in aqueous solution. *Applied Surface Sci.*, 282: 38-45.
7. Fu, F., L. Xie, B. Tang, Q. Wang and S. Jiang, 2012. Application of a novel strategy-advanced fenton-chemical precipitation to the treatment of strong stability chelated heavy metal containing wastewater. *Chem. Eng. J.*, 189: 283-287.
8. Bozecka, A., M. Orlof-Naturalna and S. Sanak-Rydlowska, 2016. Removal of lead, cadmium and copper ions from aqueous solutions by using ion exchange resin C 160. *Gospodarka Surowcami Mineralnymi*, 32: 129-140.
9. Pang, F.M., P. Kumar, T.T. Teng, A.K. Mohd Omar and K.L. Wasewar, 2011. Removal of lead, zinc and iron by coagulation-flocculation. *J. Taiwan Inst. Chem. Eng.*, 42: 809-815.
10. Chan, B.K.C. and A.W.L. Dudeney, 2008. Reverse osmosis removal of arsenic residues from bioleaching of refractory gold concentrates. *Minerals Eng.*, 21: 272-278.
11. Song, J., H. Oh, H. Kong and J. Jang, 2011. Poly rhodanine modified anodic aluminum oxide membrane for heavy metal ions removal. *J. Hazard. Mater.*, 187: 311-317.
12. Badruddoza, A.Z.M., Z.B.Z. Shawon, W.J.D. Tay, K. Hidajat and M.S. Uddin, 2013. Fe₃O₄/cyclodextrin polymer nanocomposites for selective heavy metals removal from industrial wastewater. *Carbohydrate Polymers*, 91: 322-332.
13. Lakherwal, D., 2014. Adsorption of heavy metals: A review. *Int. J. Environ. Res. Dev.*, 4: 41-48.
14. Smith, A., 2006. Opinion: Nanotech-The way forward for clean water? *Filtr. Sep.*, 43: 32-33.
15. Rafique, U., A. Imtiaz and A.K. Khan, 2012. Synthesis, characterization and application of nanomaterials for the removal of emerging pollutants from industrial waste water, kinetics and equilibrium model. *J. Water Sustainability*, 2: 233-244.
16. Abd El Fatah, M. and M.E. Ossman, 2014. Removal of heavy metal by nickel oxide nano powder. *Int. J. Environ. Res.*, 8: 741-750.
17. Jeon, Y.T., J.Y. Moon, G.H. Lee, J. Park and Y. Chang, 2006. Comparison of the magnetic properties of metastable hexagonal close-packed Ni nanoparticles with those of the stable face-centered cubic Ni nanoparticles. *J. Phys. Chem. B*, 110: 1187-1191.

18. Teja, A.S. and P.Y. Koh, 2009. Synthesis, properties and applications of magnetic iron oxide nanoparticles. *Prog. Crystal Growth Characteriz. Mater.*, 55: 22-45.
19. Neuberger, T., B. Schopf, H. Hofmann, M. Hofmann and B. von Rechenberg, 2005. Superparamagnetic nanoparticles for biomedical applications: Possibilities and limitations of a new drug delivery system. *J. Magn. Mater.*, 293: 483-496.
20. Mayo, J.T., C. Yavuz, S. Yean, L. Cong and H. Shipley *et al.*, 2007. The effect of nanocrystalline magnetite size on arsenic removal. *Sci. Technol. Adv. Mater.*, 8: 71-75.
21. Yavuz, C.T., J.T. Mayo, W.W. Yu, A. Prakash and J.C. Falkner *et al.*, 2006. Low-field magnetic separation of monodisperse Fe₃O₄ nanocrystals. *Science*, 314: 964-967.
22. Ai, Z., Y. Cheng, L. Zhang and J. Qiu, 2008. Efficient removal of Cr (VI) from aqueous solution with Fe@Fe₂O₃ core-shell nanowires. *Environ. Sci. Technol.*, 42: 6955-6960.
23. APHA., 2012. Standard Methods for the Examination of Water and Wastewater. 22nd Edn., American Public Health Association, USA.
24. Emara, M.M., M.E. Goher, M.A. Abdo, N.M. Mahmod and A.E. El-Shamy, 2016. Synthesis and characterization of Fe, Mn and super paramagnetic magnetite Fe₃O₄ nanoparticles. *Int. J. Adv. Res.*, 4: 447-461.
25. Rahman, N. and U. Haseen, 2015. Development of polyacrylamide chromium oxide as a new sorbent for solid phase extraction of As (III) from food and environmental water samples. *RSC Adv.*, 5: 7311-7323.
26. Oh, M. and M. Tshabalala, 2007. Pelletized ponderosa pine bark for adsorption of toxic heavy metals from water. *BioResources*, 2: 66-81.
27. DeMarco, M.J., A.K. SenGupta and J.E. Greenleaf, 2003. Arsenic removal using a polymeric/inorganic hybrid sorbent. *Water Res.*, 37: 164-176.
28. Srivastava, V. and Y.C. Sharma, 2013. Synthesis and characterization of Fe₃O₄@n-SiO₂ nanoparticles from an agro waste material and its application for the removal of Cr (VI) from aqueous solutions. *Water Air Soil Pollut.*, 225: 1776-1787.
29. Khalilnezhad, R., M.E. Olya, M. Khosravi and R. Marandi, 2014. Manganese biosorption from aqueous solution by *Penicillium camemberti* biomass in the batch and fixed bed reactors: A kinetic study. *Applied Biochem. Biotechnol.*, 174: 1919-1934.
30. Kamarudzaman, A.N., T.C. Chay, A. Amir and S.A. Talib, 2015. Biosorption of Mn (II) ions from aqueous solution by pleurotus spent mushroom compost in a fixed-bed column. *Procedia-Soc. Behav. Sci.*, 195: 2709-2716.
31. Gupta, S. and B.V. Babu, 2010. Experimental, kinetic, equilibrium and regeneration studies for adsorption of Cr (VI) from aqueous solutions using low cost adsorbent (activated fly ash). *Desalin. Water Treat.*, 20: 167-178.
32. Yahaya, N.K.E.M., I. Abustan, M.F.P.M. Latiff, O.S. Bello and M.A. Ahmad, 2011. Fixed-bed column study for Cu (II) removal from aqueous solutions using rice husk based activated carbon. *Int. J. Eng. Technol.*, 11: 248-252.
33. Goher, M.E., M.H. Ali, I.A. Abdel-Moniem, A.H. Fahmy, M.H. Abdo and S.M. El-Sayed, 2015. Removal of aluminum, iron and manganese ions from industrial wastes using granular activated carbon and Amberlite IR-120H. *Egypt. J. Aquat. Res.*, 41: 155-164.
34. Goher, M.E., A.M. Abd El-Monem, A.M. Abdel-Satar, M.H.H. Ali, A.M. Hussian and A. Napiorkowska-Krzebietkec, 2016. Biosorption of some toxic metals from aqueous solution using non-living algal cells of *Chlorella vulgaris*. *J. Elementol.*, 21: 703-713.
35. Fang, X.B., Z.Q. Fang, P.K.E. Tsang, W. Cheng, X.M. Yan and L.C. Zheng, 2014. Selective adsorption of Cr (VI) from aqueous solution by EDA-Fe₃O₄ nanoparticles prepared from steel pickling waste liquor. *Applied Surface Sci.*, 314: 655-662.
36. Ho, S.H., C.Y. Chen, D.J. Lee and J.S. Chang, 2011. Perspectives on microalgal CO₂-emission mitigation systems-a review. *Biotechnol. Adv.*, 29: 189-198.
37. Agarwal, A.K., M.S. Kadu, C.P. Pandhurnekar and I.L. Muthreja, 2015. Kinetics study on the adsorption of Ni²⁺ ions onto fly ash. *J. Chem. Technol. Metall.*, 50: 601-605.
38. Gupta, S. and B.V. Babu, 2009. Removal of toxic metal Cr (VI) from aqueous solutions using sawdust as adsorbent: Equilibrium, kinetics and regeneration studies. *Chem. Eng. J.*, 150: 352-365.
39. Gupta, S. and B.V. Babu, 2009. Utilization of waste product (tamarind seeds) for the removal of Cr (VI) from aqueous solutions: Equilibrium, kinetics and regeneration studies. *J. Environ. Manage.*, 90: 3013-3022.
40. Gimbert, F., N. Morin-Crini, F. Renault, P.M. Badot and G. Crini, 2008. Adsorption isotherm models for dye removal by cationized starch-based material in a single component system: Error analysis. *J. Hazard. Mater.*, 157: 34-46.
41. Subramanyam, B. and A. Das, 2009. Linearized and non-linearized isotherm models comparative study on adsorption of aqueous phenol solution in soil. *Int. J. Environ. Sci. Technol.*, 6: 633-640.
42. Bhargavi, R.J., U. Maheshwari and S. Gupta, 2015. Synthesis and use of alumina nanoparticles as an adsorbent for the removal of Zn (II) and CBG dye from wastewater. *Int. J. Ind. Chem.*, 6: 31-41.